A Video Traffic Model based on the Shifting-Level Process: the Effects of SRD and LRD on Queueing Behavior

Heejune Ahn, Reseach Center LGIC Ltd.
Jae-Kyoon Kim, Dept. Electircal Eng. KAIST
Song Chong, Dept Electrical Eng. Sogang Univisity
Bara Kim, and Bong Dae Choi, Dept. of Mathematics Korea University

Abstract— **Recently, a number of empirical studies have demonstrated the existence of long-range dependence (LRD) or self-similarity in VBR video traffic. Since previous LRD models cannot capture all short- and long-term correlation and rate-distribution while still retaining mathematical tractability, there exist many doubts on the importance of SRD, LRD, and rate-distribution on traffic engineering.**

In this paper, we present a video traffic model based on the *shifting-level (SL) process* with an accurate parameter matching algorithm for video traffic. The SL process captures all those key statistics of an empirical video trace. Also, we devised a queueing analysis method of SL/D/1/K, where the system size at every embedded point is quantized into a fixed set of values, thus name *quantization reduction method*. This method is different from previous LRD queueing results in that it provides queueing results over all range not just an asymptotic solution. Further, this method provides not only the approximation but also the bounds of the approximation for the system states and thus guarantees the accuracy of the analysis.

Especially, we found that for most available traces their ACF can be accurately modeled by a compound correlation (SLCC): an exponential function in short range and a hyperbolic function in long range. Comparing the queueing perforamces with C-DAR(1), the SLCC, and real video traces identifies the *effects of SRD and LRD* in VBR video traffic on queueing performance.

Keywords— **VBR video traffic model, shifting-level process (SL), autocorrelation, long-range dependence (LRD), short-range dependence (SRD), queueing analysis.**

I. Introduction

VBR video service is expected to be a major source of future packet-switching integrated service networks. Because the success of traffic control relies essentially on a sound understanding of input traffic, modeling of VBR video traffic has received intense interest. Of input traffic statistics, the histogram (rate-distribution) and the autocorrelation function (ACF) are considered of first importance in estimating network performances [13], [14], [20], [25].

Recently, a number of empirical studies have demonstrated the existence of long-range dependence (LRD) or self-similarity in VBR video traffic [5], [11], [12]. Various processes have been proposed for modeling a traffic with LRD and analyzing its effects on network performance [5] and [25] pp.324-348. These include fractional Brownian motion [11], [24], fractional ARIMA processes [17], chaotic maps [8], and semi-Markovian processes [18]. The significant impact of LRD on queueing behavior has been reported in their studies on data traffic. Erramilli [9] and Norros [24] showed that overall packet loss decreases very slowly, i.e., hyperbolically with increasing buffer size. This means that system performance may be overestimated if LRD in input traffic is overlooked. However, since previous LRD models cannot capture all short- and long-term correlation and rate-distribution while still retaining mathematical tractability, there exist many doubts on the importance of SRD, LRD, and rate-distribution on traffic engineering. Also, conventional Markovian models are still being used and developed for performance estimation and traffic control. Furthermore, it is argued that Markovian models show accurate performance estimation in many situations in spite of a lack of LRD characteristics [6], [16].

In this paper, we introduce a video traffic model based on the ***shifting-level (SL) process***. The SL process was first studied in an economics context and called a ***renewal reward process*** by Mandelbrot [22]. An application to video traffic was done by Grasse ***et al.*** [12]. Roughly speaking, the SL process is a traffic model for a source that changes its rate now and then according to two i.i.d. processes: S_i for scene size (the arrival rate in a scene) and T_i for scene duration. As we will describe, because in the SL process, the histogram and ACF can be matched independently, the effects of each statistic on queueing performance can be investigated separately. With the assumption of a negative binomial distribution on the histogram, obtained from previous studies [6], [11], [15], we focus on the effect of autocorrelation on queueing behavior.

We observe that the ACF of an empirical trace is accurately captured by the shifting-level process with a compound correlation of the exponential and the hyperbolic, which we will refer to as the ***shifting-level process with compound correlation*** (SLCC). Especially, we present an efficient and accurate parameter matching algorithm for the SLCC model from a measured video traffic. The continuous-time analog (C-DAR(1)) of DAR(1) model [15],

This work was done when H. Ahn, B. Kim, and B. D. Choi were with KAIST (Korea Advanced Institute of Science and Technology). This work was supported in part by Korea Science and Engineering Foundation (KOSEF) under Grant 98-0101-02-01-3. The corresponding author is H. Ahn (The Centeral R&D Center, LG Information & Communications (LGIC) Ltd., 533 Hokye-dong, Anyang-si, Korea, e-mail: cityboy@viscom.kaist.ac.kr).

[29], which is a widely used SRD video traffic model, can be considered a kind of SL process but with only an exponential correlation. Therefore, by comparing the queueing performances of the C-DAR(1) model and SLCC with that of a real video trace, we will identify the effects of SRD and LRD correlation in VBR video traffic on queueing performance.

We present an approximating method named the ***quantization reduction method***, where the system sizes at embedded points, i.e., the rate transition epochs of the SL process, are approximated into a space with a finite number of quantization points. This method is different from previous LRD queueing results in that it provides queueing results over all range not just an asymptotic solution. Since we provide also the upper and lower bounds of the approximation for the system size distribution, we can efficiently use the memory size and computation time by adjusting the quantization step.

As an important final note, due to space limitations, we do not provide all detailed equations and extensive results obtained with various traces. However, we applied our modeling and alogorithm to various traces, JPEG-coded ***Star Wars*** [11], VIC traces [28], and GOP smoothed MPEG [18], [26]. Interested readers for more numerical results are refered to the refernce [2].

The rest of the paper is structured as follows. In Section II, we introduce the SL process and find its autocorrelation. In Section III, we propose a parameter matching method of the SLCC for ACF with exponential and hyperbolic form. In Section IV, we offer an analysis method for the SL/D/1/K queueing system. The numerical results on queueing experiments are presented in Section V. Finally we conclude the work in Section VI.

II. The Shifting-Level Process

A. The Shifting-Level Process and its ACF

Let $\{S_n : n = 0, 1, 2, 3\}$ be i.i.d. discrete random variables with a state space $\{0, 1, 2, \cdots, i, \cdots, M\}$. We denote the probability mass function, mean, and variance of S_n by $f_S(\cdot)$, μ_S, and σ_S^2, respectively. Consider a delayed renewal process $0 = t_0 < t_1 < t_2 < \cdots$ with inter-renewal times $T_n = t_n - t_{n-1}, n = 1, 2, 3 \cdots$, where $\{T_n : n = 2, 3, 4 \cdots\}$ are i.i.d. with distribution $F_T(\cdot)$, density $f_T(\cdot)$, and mean μ_T, and T_1 follows $F^e(t)$, the distribution for a residual life time of T [27]:

$$F_T^e(t) = \frac{1}{\mu_T} \int_0^t (1 - F_T(x))dx. \tag{1}$$

Then the ***shifting-level process*** $\{X(t)\}$ is a fluid model whose arrival rate at t is given by i if $S_{N(t)} = i$;

$$X(t) = \sum_{n=0}^{\infty} S_n 1_{\{t_n \le t < t_{n+1}\}}. \tag{2}$$

Obviously, $\{X(t)\}$ is a stationary process with mean $\mu_X = \mu_S$ and variance $\sigma_X^2 = \sigma_S^2$.

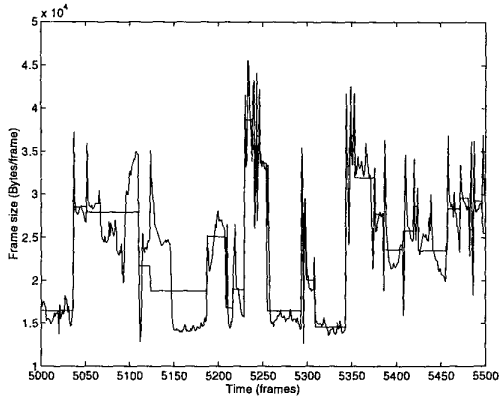

Fig. 1. A sample path for the SLCC with the same ACF and the marginal distribution as the intra-coded ***Star Wars*** trace

Now we find the relationship between the ACF $\rho(t) = E[(X(\tau) - \mu_X)(X(\tau + t) - \mu_X)]/Var[X(t)]$ and the scene duration distribution $F_T(\cdot)$. First the ACF of the SL process is given by

$$\rho(t) = \frac{1}{\mu_T} \int_t^{\infty} (1 - F_T(y))\, dy. \tag{3}$$

The derivation of equation (3) is provided in the Appendix A.

Differentiation of the equation yields simple relations between the density of T and the ACF.

$$F_T(t) = 1 + \mu_T \rho'(t), \tag{4}$$

and

$$f_T(t) = \mu_T \rho''(t). \tag{5}$$

B. The SL process as a Video Traffic Model

Now we consider application of the SL process to video traffic modeling. In general, the traffic pattern of a coded video trace depends on both the inherent variation of the visual information and the coding algorithm used for data compression. Especially, an MPEG coder generates periodic burstiness due to its picture-dependent coding algorithm. Here we focus on the inherent characteristics in VBR video traffic, no considering the side-effects of video coding, i.e., the periodicity of MPEG traffic. Table I shows the basic statistics for the traces used in our experiment. Here we assume 48 Bytes payload in 53 Bytes ATM cell size.

In our application, the scene size, i.e., the source rate in a scene, corresponds to S_i and the scene duration corresponds to T_i. In general, the scene size process might not be i.i.d.; the real correlation depends on the definition of scene. In [18], the correlation is modeled by a discrete Markov chain. However, the large number of parameters in the transition matrix of semi-Markovian processes makes

TABLE I

STATISTICS FOR THE TRACES USED IN OUR EXPERIMENT (CELLS/FRAME OR CELLS/GOP

trace	mean	std.	coef. of var.	peak	peak/mean
intra-coded *Star Wars*	578.9	130.2	0.23	1,634.6	2.82
VIC *Trace A*	85.2	61.3	0.72	433.5	5.09
VIC *Trace B*	71.9	39.0	0.82	544.3	7.57
MPEG-GOP smoothed	589.1	331.6	0.56	3,796.7	6.44

the matching procedure difficult. Furthermore, the performance estimation is very sensitive to its state definition [18]. This is because semi-Markovian models cannot capture the rate-distribution (first-order statistics) of the empirical traces with a limited number of states.

On the other hand, in the SL process assuming that the scene size process is also a renewal process, the SL process has the property that the marginal distribution and the ACF are determined solely by S_i and T_i, respectively. Thus, we can easily match the rate-distribution and ACF of the model to those of the empirical traces. Furthermore, as we will show, our modeling of ACF based on the SL process requires only five parameters for VBR video traffic.

C. The SLCC and the C-DAR(1) model

Fig. 2 shows that the empirical ACF of video traffic is close to an exponential function (SRD) in the small lag region, and a hyperbolic function (LRD) in the large lag region. Thus, we consider the ***shifting-level process with a compound correlation (SLCC)*** of the exponential and the hyperbolic as follows.

$$\rho(t) = \begin{cases} \rho_e(t) = e^{-t/\tau}, & \text{for } 0 < t < t_0, \\ \rho_h(t) = c_0(t+t_1)^{-\beta}, & \text{for } t_0 < t \end{cases} \quad (6)$$

First, we obtain $\rho_e'(t) = -e^{-t/\tau}/\tau$, and $\rho_h'(t) = -c_0\beta\,(t+t_1)^{-(\beta+1)}$. Then from (5) we find that T must also follow the exponential and hyperbolic distribution. Fig. 1 shows a sample trace of the SLCC process whose model parameters are matched with a ***Star Wars*** trace [11] using the parameter matching algorithm in Section III.

Here we consider the relationship between the SLCC process and the well-known DAR(1) model [15]. The DAR(1) model is a Markov chain with transition matrix

$$\mathbf{P} = \rho\mathbf{I} + (1-\rho)\mathbf{Q}, \quad (7)$$

where ρ is the autocorrelation coefficient and $\mathbf{Q}$ is a state transition matrix with identical rows equal to the marginal distribution $f_S(\cdot)$.

To compare the DAR(1) model with the SL process, which is a continuous-time model, we consider the continuous-time analog (C-DAR(1)) of the DAR(1) model, which was named and studied in [29]. The motivation of the DAR(1) model is not discrete-time modeling but accurate modeling of the marginal distribution in an empirical

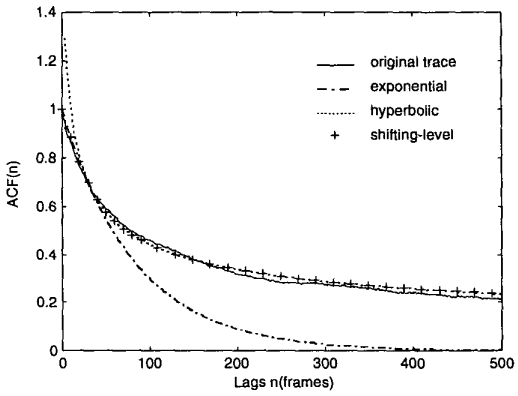

Fig. 2. ACFs for original, exponential, hyperbolic and SLCC

trace [15], [29]; the original AR(1) model follows a Gaussian distribution. Furthermore, the exact match of DAR(1) and C-DAR(1) has been verified in [29]. The C-DAR(1) model is a kind of SLCC process with exponential autocorrelation only in the SLCC, i.e., $\rho(t) = e^{-t/\tau}$.

The C-DAR(1) model is a SRD process ($\sum \rho(t) < \infty$), and cannot capture the heavy-tail properties in ACF of real video traffics. On the other hand, the SLCC is a LRD process ($\sum \rho(t) = \infty$). Since the SLCC and the C-DAR(1) model have the same rate-distribution and short-term correlation structure except the hyperbolic tail, comparing the queueing performances of them will reveal the effects of long-range dependence in video traffic.

III. PARAMETER MATCHING OF THE SL PROCESS

A. The Proposed Parameter Matching Algorithm

Now we consider an algorithm which matches the parameters of the SLCC to the statistics of a real video traffic. In the SL process, the histogram is determined by the scene size S_i, and the ACF is determined by the scene duration T_i.

First, we propose the matching procedure for the ACF of the SLCC process. To approximate the ACF of a real video sequence by $\rho(t)$ given in (6), we have to determine the values of 5 parameters τ, β, t_0, t_1, and c_0. We obtain

the exponential decaying rate τ using

$$\tau = -t/\ln(\rho(t)), \tag{8}$$

where we use $t = 10$ frames, and the hyperbolic decaying rate

$$\beta = 2 - 2H \tag{9}$$

by the Hurst parameter estimation [5]. For parameters c_0 and t_0, we further assume that the ACF $\rho(t)$ and the distribution function $F_T(t)$ are ***continuous***, especially at t_0. Then, we obtain the two relations:

$$\rho_e(t_0) = \rho_h(t_0) \text{ and } \rho_e'(t_0) = \rho_h'(t_0). \tag{10}$$

That is, $e^{-t_0/\tau} = c_0(t_0+t_1)^{-\beta}$ and $-\frac{1}{\tau}e^{-t_0/\tau} = c_0(-\beta)(t_0+t_1)^{-(\beta+1)}$.

Solving the system of equations above, we finally obtain

$$t_0 = \beta\tau - t_1 \tag{11}$$

$$c_0 = (\tau\beta)^{\beta}e^{-(\beta - t_1/\tau)}. \tag{12}$$

The fifth paramter t_1 is introduced in order to model the ACF of a real video traffic with preserving the continuity properties of $\rho(t)$ and $F_T(t)$. Because t_0 and c_0 are functions of t_1, we use a least square fitting to determine the parameter t_1. We use the method of Hooke and Jeeves with discrete steps [4], to find t_1 that minimizes the square-error of the autocorrelation function

$$LSE(t_1) = \sum_{n=0}^{n_{\max}} [\rho(n) - \rho_R(n)]^2, \tag{13}$$

where $\rho_R(n)$ and $n_{\max}$ denote the ACF for a real trace and the summation range of calculation, respectively. The search range of t_1 is $[0, \beta\tau]$, because $t_0 > 0$ and equation (11). For numerical calculation, we use a value of 500 frames for $n_{\max}$. Furthermore, from the relation $f_T(t) = \mu_T\rho''(t)$, and $\int_0^{\infty} f_T(t)dt = 1$, we obtain $\mu_T = \tau$.

For the random number generation, we here obtain the distribution function for the compound ACF model.

$$F_T(t) = \begin{cases} 1 - e^{-t/\tau}, & \text{for } t < t_0, \\ 1 - \tau\beta c_0(t + t_1)^{-(\beta+1)}, & \text{for } t_0 \le t \end{cases} \tag{14}$$

and the inverse of $F_T(\cdot)$ is given by

$$F_T^{-1}(y) = \begin{cases} -\tau\ln(1-y), & \text{for } y < 1 - e^{-\beta+t_1/\tau} \\ \left(\frac{\beta c_0\tau}{1-y}\right)^{\frac{1}{\beta+1}} - t_1, & \text{for } y \ge 1 - e^{-\beta+t_1/\tau}. \end{cases} \tag{15}$$

The probability mass function for frame size $(f_S(0), f_S(1), \cdots, f_S(M-1), f_S(M))$ is modeled by the negative binomial distribution from the observations in [11], [15].

$$f_S(i) = \binom{-r}{i} p^r(-q)^i = \binom{i+r-1}{i} p^r q^i, \tag{16}$$

$(i = 0, 1, 2, \cdots, M-1)$ and $f_S(M) = 1 - \sum_{i<M} f_S(i)$, where M is the peak rate in cells per frame.

The mean and variance of this distribution are

$$E[X(t)] = \frac{r(1-p)}{p} \quad \text{and} \quad Var[X(t)] = \frac{r(1-p)}{p^2}, \tag{17}$$

respectively. Here, $0 < p < 1$, $q = 1 - p$, and $r > 0$. Thus, the parameters are obtained by

$$p = \frac{E[X(t)]}{Var[X(t)]} \quad \text{and} \quad r = \frac{E[X(t)]^2}{Var[X(t)] - E[X(t)]}. \tag{18}$$

Here we summarize the parameter matching procedure:
For F_T,

- Obtain τ by equation (8), and β by equation (9).
- Obtain t_0, c_0 and t_1 from the least square fitting and the relationship (11) and (12).

For f_S,

- Obtain p, r by equations (18).

B. Numerical Results with Empirical Traces

The parameters of the SLCC is obtained as follows. First, since the derivations in Section 3 are continuous-time versions, we round off scene durations into integer numbers. First, for the JPEG coded ***Star Wars*** traces: for the ACF, $\tau = 82.83$ frames, $\beta = 0.39$, $t_0 = 30.13$ frames, $t_1 = 3.0$ frames, and $c_0 = 2.82$, and for the histogram, $M = 1{,}634$ cells, $E[X(t)] = 578.9$ cells/frame, and $\sqrt{Var[X(t)]} = 130.2$ and thus $p = 0.0341$ and $r = 20.44 \sim 20$ are obtained. In the same way, we obtained the parameters for various traces, ***vic trace A***, ***vic trace B***, and ***GOP-smoothed MPEG*** the same way, and verified the performance of our modeling (Fig. 3): For the vic ***trace A***, $t_0 = 12.4361$ frames, $t_1 = 1$ frames, $\beta = 0.63$, $c_0 = 2.8679$, $a = 0.9542$, and $\tau = 21.3272$ frames. For the vic ***trace B***, $t_0 = 3.2950$ frames, $t_1 = 10$ frames, $\beta = 0.3500$, $c_0 = 2.2679$, $a = 0.9740$, and $\tau = 37.9856$ frames. For the ***GOP smoothed MPEG***, $t_0 = 1.33$ GOPs, $t_1 = 1$ GOPs, $\beta = 0.26$, $c_0 = 1.0741$, $a = 0.8944$ GOPs, and $\tau = 8.9615$ GOPs (with a GOP size of 12 frames). For the corresponding C-DAR(1) models, we use the same value of τ (for the exponential decay rate), and p and r (for the histogram) as for the SLCC process. For more detailed results, see [2].

Now we examine how accurately the SLCC model emulates the ACF of the empirical traces. Figs. 2 and 3 shows four ACFs: (a) original, (b) exponential, (c) hyperbolic, and (d) the SLCC. The SLCC from the proposed parameter matching algorithm provides a very good fit at both the small and large lags, while the exponential curve of the C-DAR(1) underestimates in the region of large lags. Therefore, with the assumption that negative binomial distribution accurately matches the frame size distribution, we can conclude that the statistical characteristics of the SL process are quite close to those of the original video trace up to second-order statistics.

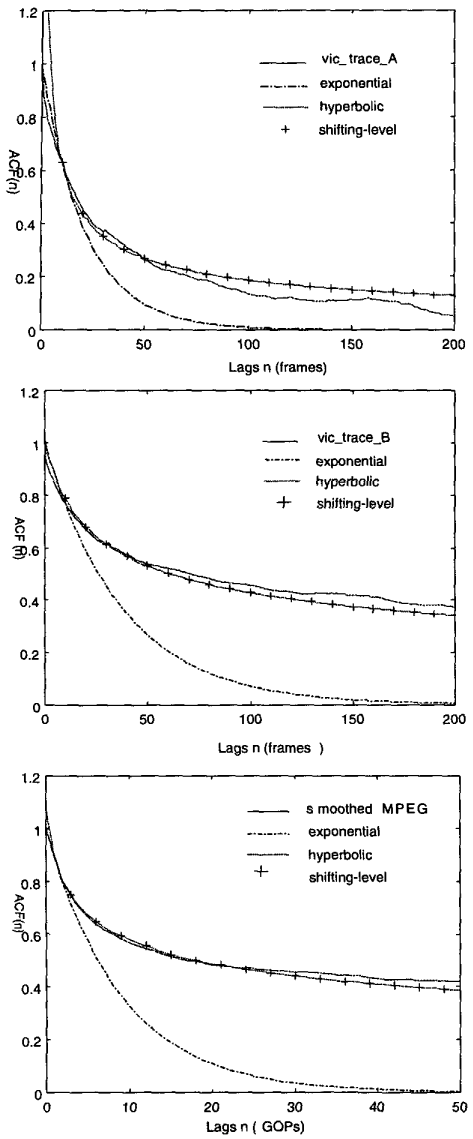

Fig. 3. ACFs for original, exponential, hyperbolic and SLCC (VIC Trace A, VIC trace B, GOP smoothed MPEG)

IV. An Efficient Analysis of the SL/D/1/K Queueing System

A. The Quantization Reduction Method

In this section, we present an efficient analysis method for the SL/D/1/K queueing system. We consider a single server fluid queueing system with a buffer of size K cells and a deterministic service rate of C cells per frame. Input arrives at rate i, when the SLCC process $X(t)$ is state i at time t. Let $L(t)$ be the number of cells in the system at time t. We are interested in the stochastic process $\{X(t), L(t), t \geq 0\}$, which characterizes the dynamics of the system. Let t_n is the state transition epoch of the SL process. Then $\{(X_n, L_n) \equiv (X(t_n^+), L(t_n^+))\}$ is an embedded Markov chain. However, the exact analysis of this system is very difficult, because L_n takes a continuous value in $[0, K]$ and the sojourn times of states in a SL process do not follow an exponential distribution. Therefore, we present an approximation method, which we call ***quantization reduction method***, to approximate the system behaviors. The idea of the state space quantization method is to reduce the state space of a continuous queue size L_n, $[0, K]$ to a finite set of quantization points $\{0, h, 2h, \cdots, Dh = K\}$, where h is the quantization step and $D+1$ is the number of the queue states.

First, we define 3 auxiliary processes $L^u(t)$, $L^a(t)$ and $L^l(t)$ for $L(t)$. The superscripts u,a, and l mean upper bound, approximation, and lower bound, respectively. At every transition epoch of input, t_n, the processes, $L^u(t)$, $L^a(t)$, and $L^l(t)$ are approximated by their respective quantizers: $L_n^u \equiv L^u(t_n^+) = \mathcal{F}^u(L^u(t_n^-))$, $L_n^a \equiv L^a(t_n^+) = \mathcal{F}^a(L^a(t_n^-))$, and $L_n^l \equiv L^l(t_n^+) = \mathcal{F}^l(L^l(t_n^-))$. These quantization functions are all staircase functions (Fig. 4) and given as follows.

$$\mathcal{F}^a := \begin{cases} [0, \frac{h}{2}) \to 0 & l = 0, \\ [lh - \frac{h}{2}, lh + \frac{h}{2}) \to lh, & l = 1, 2, \cdots D-1, \\ [Dh - \frac{h}{2}, K] \to Dh & l = D. \end{cases} \tag{19}$$

$$\mathcal{F}^u := \begin{cases} 0 \to 0, & l = 0, \\ ((l-1)h, lh] \to lh, & l = 1, 2, \cdots D. \end{cases} \tag{20}$$

$$\mathcal{F}^l := \begin{cases} [lh, (l+1)h) \to lh, & l = 0, 1, 2, \cdots D-1, \\ Dh \to Dh, & l = D. \end{cases} \tag{21}$$

Fig. 5 illustrates a sample path for each stochastic process, L_n^u, L_n^a, L_n^l, and L_n, and $L_n^u(t)$,$L_n^a(t)$, $L_n^l(t)$, and $L_n(t)$, to show the relationship among them. Since $L_0^l \leq L_0^a \sim L_0 \leq L_0^u$ and 4 systems are loaded by the same SL input, it is clear that $L_n^l \leq L_n^a \sim L_n \leq L_n^u, i = 1, 2, 3, \cdots$. And, it is also clear that $L^l(t) \leq L^a(t) \sim L(t) \leq L^u(t)$.

The processes $\{X_n, L_n^a\}$, $\{X_n, L_n^u\}$, and $\{X_n, L_n^l\}$ are all irreducible and positive recurrent embedded Markov chains and thus the queuing analysis is based on the transition matrix of the embedded processes. Let $\mathbf{P}^a$,$\mathbf{P}^u$, and $\mathbf{P}^l$ be the one-step transition probability matrix of $\{(X_n, L_n^a)\}$, $\{(X_n, L_n^u)\}$, and $\{(X_n, L_n^a)\}$, respectively. The elements of the transition matrices $(c = u, a, l)$ are defined by

$$p^c_{(i,l),(j,k)} \equiv Pr\{(X_{n+1}, L^c_{n+1}) = (j, kh) | (X_n, L^c_n) = (i, lh)\}, \tag{22}$$

Noting that during $[t_n, t_{n+1})$, input arrives at uniform rate of i cells per frame, the elements of each transition matrix is obtained as Appendix B.

We define the limiting probabilities

$$\pi^c_{i,l} = \lim_{n \to \infty} Pr[(X_n^c = i, L_n^c = lh)], c = u, a, l.$$

Then the limiting probability vector $\pi^c = (\pi^c_{0,0}, \pi^c_{0,1}, \cdots, \pi^c_{0,D}, \pi^c_{1,0}, \cdots \pi^c_{M,D})$ is uniquely determined by

$$\pi^c P^c = \pi^c \text{ and } \pi^c e^T = 1, c = u, a, l, \quad (23)$$

where e is a unity vector of dimension $(D+1)(M+1)$.

The computation can be obtained using standard numerical methods for solving system of equations. However, substantial saving in computation can be obtained if the renewal property of the SL process is used. First, we obtain a new transition matrix $\hat{\mathbf{P}}^c, c = u, a, l$ by merging the elements of the original transition matrix $\mathbf{P}^c$,

$$\hat{p}^c_{l,k} = \sum_{i,j} p^c_{(i,l),(j,k)} \quad (24)$$

and then solve the system of equations,

$$\hat{\pi}^c \hat{\mathbf{P}}^c = \hat{\pi}^c \text{ and } \hat{\pi}^c \mathbf{e}^T = 1, c = u, a, l, \quad (25)$$

where e is a unitary vector of dimension $D+1$. Finally, the steady-state probability $\pi^c_{i,l}$ is obtained by producting the probability of rates,

$$\pi^c_{i,l} = f_S(i) \cdot \hat{\pi}^c_l, c = u, a, l. \quad (26)$$

This observation reduces the dimension of the matrix from $(D+1)(M+1) \times (D+1)(M+1)$ into $(D+1) \times (D+1)$.

We now obtain the survival function, i.e., the complementary queue distribution at arbitrary times, and cell loss probability as performance measures. Since $L^l(t) \leq L^a(t) \sim L(t) \leq L^u(t)$, it is also clear that $Pr[L^l(t) < x] \leq Pr[L^a(t) > x] \sim Pr[L(t) > x] \leq Pr[L^u(t) > x]$ for $x \geq 0$ and $CLP^l \leq CLP^a \sim CLP \leq CLP^u$. The survival function $Pr[L(t) > x]$ is obtained by calculating T_a the fraction of time when the $L(t)$ stays above system size x between two successive embedded points, t_n and t_{n+1}:

$$Pr[L^c(t) > x] = \frac{\sum_s \sum_l \pi^c_{i,l} E(T_a(x)|(i,l))}{E(T)}, \quad c = u, a, l \quad (27)$$

where the conditional expectation $\bar{T}(x) = E(T_a(x)|(i,l))$ is obtained by

$$\bar{T}(x) = \begin{cases} E(T) & \text{for } i \geq C, lh \geq x \\ E((T - \frac{x-lh}{i-C})^+|(i,l)) & \text{for } i \geq C, lh < x \\ E((\frac{lh-x}{C-i} - T)^+|(i,l)) & \text{for } i < C, lh > x \\ 0 & \text{for } i < C, lh \leq x \end{cases} \quad (28)$$

The cell loss probabilities $CLP^c, c = u, a, l$ are defined by the fraction of overflow data among the total arrivals. Noting that overflow occurs only when the input rate is larger than C, we obtain

$$CLP^c \equiv \frac{\sum_{i>C} \sum_l \pi^c_{i,l} (i-C) E(\left(T - \frac{K-hl}{i-C}\right)^+ |(i,l))}{E(T)E(S)}, \quad (29)$$

$(c = u, a, l)$.

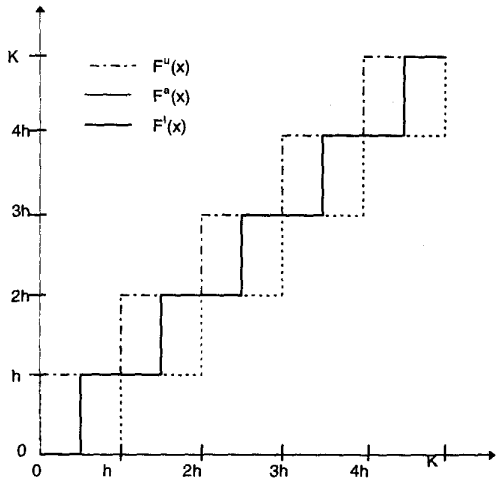

Fig. 4. The quantization functions: $\mathcal{F}^a$, $\mathcal{F}^u$, and $\mathcal{F}^l$ (when $D = 5$).

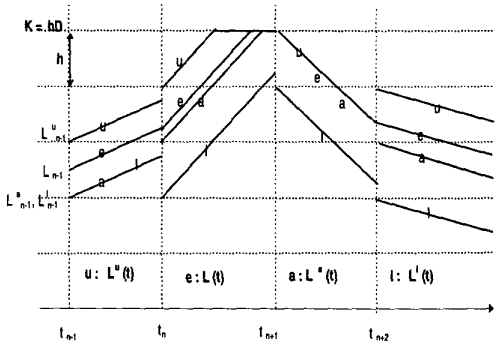

Fig. 5. Sample pathes for the $L(t)$, $L^a(t)$, $L^u(t)$, and $L^l(t)$ (when $D = 5$.

B. The Efficiency of the Quantization Reduction Method

We present the numerical results verfying the acuracy and efficiency of the quantization reduction method. However, we provide only cell loss ratio with JPEG coded ***Star Wars*** trace (for more results, see [2]).

The accuracy of the quantization reduction analysis depends on the input traffic: roughly speaking, as the product of its mean sojourn time and mean arrival rate increases, the accuracy also increases for the fixed quantization value. To verify the accuracy in video traffic application, we show numerical results for queue occupancy distributions and cell loss probabilities, varying the traffic intensity $U = 0.8$ (heavy load), $U = 0.6$ (moderate load), and $U = 0.4$ (light load).

We show the cell loss ratio for $U = 0.8, 0.6, 0.4$ and two quantization values $h_1 = 5000, h_2 = 500$ cells, in Tables II, III, and IV. The error bounds of cell loss ratio, $\epsilon = CLP^u - CLP^l$, are tighter than those for queue occupancy. It was expected from that quantization reduction method estimates more accurately at large queue sizes [2].

From these results, we conclude that the quantization reduction method is efficient and accurate in the queueing performances for VBR video traffic. Therefore, in the next section, although we show only the result of L^a with quantization value h_2, for simplicity, the results are obtained within accuracy of 1%.

Our quantization reduction method has the important advantage that the range of error of the approximation $L^a(t)$ from $L(t)$ is given by providing the the upper and lower bounds from the auxiliary processes $L^u(t)$ and $L^l(t)$. And thus we can efficiently use the memory size and computation time for performance measures by adjusting the quantization step. Furthermore, in the SL process we do not suffer from computational load since the dimension of the one-step transition matrix $\hat{\mathbf{P}}^c, c = u, a, l$ does not depend on the size of the state space for input process. Thus we can accurately match the histogram (first-order statistics) of an input process without a significant increase in the computational load.

V. Queueing Performance Results

Now we conduct several queueing experiments: for a single stream, and for statistically multiplexed streams. The purpose of these experiments is to compare the queueing behaviors of the SLCC and the C-DAR(1) model with that of an empirical trace, so that we determine under what condition LRD is crucial for queueing behavior.

First, we examine the queueing behavior for a single source varying the input traffic load. The queueing performances loaded with the SLCC and the C-DAR(1) model are obtained by the quantization reduction method (h_2). For simulation with the original trace, we start the trace at a random number of frames, and upon reaching the end of the trace, wrap each source around to the beginning, so all 171,000 frames are used. We conduct simulation using the iterative equation $L_{n+1} = \min(\max(L_n + X_n - C, 0), K)$.

A summary of queue size distributions and cell loss probabilities with a single source for traffic load (U) 0.8 (heavy load), 0.6 (moderate load), and 0.4 (light load) is shown in Figs. 6 and 7, respectively. Note that in the region where the C-DAR(1) provides accurate prediction, the merit of SLCC process, i.e., the effects of LRD could not be observed. For the queue distribution, we use a buffer size of 50,000 cells. Detailed investigation of the figures shows that both the C-DAR(1) model and the SLCC provide acceptable prediction (in order of magnitude) in the small buffer region. Interestingly, the C-DAR(1) model significantly underestimates in the region of $U = 0.8$ and a large queue size, whereas the SL process provides accurate prediction consistently.

We now consider the effects of multiplexing independent sources. In the SL model, the parameter matching and queueing analysis for the superposed stream are straightforward from the fact that the autocovariance function of the superposed stream with N independent sources is the same as that of single sources [27] (thus the same T_n as in single sources). And we obtain the distribution of S_n by N times convolution of the distribution of the single source. In Table V, cell loss probabilities for the number of sources 5 and 10 are investigated with traffic load U = 0.8. To clearly show the changes of effect of LRD in multiple-scale buffer sizes, we divide the table into three sections: small ($K \leq 1,000$ cells), medium ($1,000 < K \leq 10,000$ cells), and large ($10,000 < K \leq 100,000$ cells) sizes. We use $h = 100, 1000$, and 2000 cells for the small, medium, large buffer sizes, respectively. Because of the smoothness due to multiplexing, the effects of hyperbolic correlation (LRD) in the SLCC does not appear clearly in small and medium size region. On the other hand, at large buffer sizes we again find significant difference in cell loss probabilities of the SLCC and the C-DAR(1). However, we defer a definite conclusion for real traffic, since we cannot obtain stable values for the cell loss probability of the empirical trace in less than 1.0E-5.

Major conclusions that can be drawn from the numerical results in this section are as follows: The SLCC provides accurate and consistent estimation for queueing performance measures, and thus histogram and ACF play a key role in queueing behavior. And the C-DAR(1) model, which does not capture the long-term correlation (LRD) structure of video traffic, also estimates fairly well in light and moderate traffic load and even heavy traffic load with multiplexing video sources. The difference in the queueing results at heavy and light traffic loads can be explained as follows. The queueing system buffers the input arrival stream and thus memorizes its correlation. At a heavy traffic load, the busy period is long enough for the queueing system to be effected by LRD of the input traffic. However, whenever the queue size hits the bottom, i.e., $L(t) = 0$, the queue state is reset and forgets the past correlation of the input stream. In contrast, The resetting event occurs more frequently as the traffic load decreases. Thus, at light traffic load long term correlation in input traffic does not have a significant impact on the queuing behavior. A similar argument can be found in [16], [7]. More specifically, in [1] we develpoed a new concept, named ***cutoff interval.*** We showed that the cutoff interval is the upper bound of time scales of input correlation that affects queue buildup and it is a monotonically increasing function of traffic load. Further, we exmained the practical ranges of cutoff interval for real video traces.

VI. Conclusions

In this work we investigated the effects of SRD and LRD components in VBR video traffic on queueing performance. We observed that the ACF of an empirical trace is accurately captured by a compound function of the exponential and hyperbolic. To differentiate the effects of the exponential (SRD) and hyperbolic correlation (LRD), we constructed the shifting-level process with compound correlation (SLCC) and presented an efficient and accurate parameter matching algorithm. Especially, the C-DAR(1)

TABLE II

CELL LOSS PROBABILITIES FOR $L^u(t)$, $L^a(t)$, AND $L^l(t)$ (U=0.8)

x	CLP $L^u(t)$		CLP for $L^a(t)$		CLP for $L^l(t)$	
(Kcells)	h_1	h_2	h_1	h_2	h_1	h_2
0	1.9287E-2	1.9287E-2	1.9287E-2	1.9287E-2	1.9287E-2	1.9287E-2
10	1.0427E-2	9.2910E-3	9.2910E-3	9.2420E-3	9.0234E-3	9.2016E-3
20	7.6814E-3	7.0617E-3	7.0555E-3	7.0354E-3	6.9085E-3	7.0133E-3
30	6.3626E-3	5.9833E-3	5.9775E-3	5.9664E-3	5.8816E-3	5.9522E-3
40	5.5759E-3	5.3169E-3	5.3121E-3	5.3048E-3	5.2423E-3	5.2946E-3
50	5.0428E-3	4.8516E-3	4.8476E-3	4.8423E-3	4.7933E-3	4.8344E-3

TABLE III

CELL LOSS PROBABILITIES FOR $L^u(t)$, $L^a(t)$, AND $L^l(t)$ (U = 0.6)

x	CLP $L^u(t)$		CLP for $L^a(t)$		CLP for $L^l(t)$	
(Kcells)	h_1	h_2	h_1	h_2	h_1	h_2
0	1.3163E-3	1.3163E-3	1.3163E-3	1.3163E-3	1.3163E-3	1.3163E-3
10	6.6359E-4	6.6205E-4	6.6199E-4	6.6196E-4	6.6142E-4	6.6187E-4
20	5.0984E-4	5.0918E-4	5.0915E-4	5.0914E-4	5.0886E-4	5.0910E-4
30	4.3527E-4	4.3490E-4	4.3488E-4	4.3488E-4	4.3470E-4	4.3485E-4
40	3.8874E-4	3.8850E-4	3.8848E-4	3.8848E-4	3.8836E-4	3.8846E-4
50	3.5598E-4	3.5580E-4	3.5578E-4	3.5578E-4	3.5569E-4	3.5577E-4

TABLE IV

CELL LOSS PROBABILITIES FOR $L^u(t)$, $L^a(t)$, AND $L^l(t)$ (U=0.4)

x	CLP $L^u(t)$		CLP for $L^a(t)$		CLP for $L^l(t)$	
(Kcells)	h_1	h_2	h_1	h_2	h_1	h_2
0	1.1704E-5	1.1704E-5	1.1704E-5	1.1704E-5	1.1704E-5	1.1704E-5
10	5.0632E-6	5.0631E-6	5.0631E-6	5.0631E-6	5.0631E-6	5.0631E-6
20	3.8651E-6	3.8651E-6	3.8651E-6	3.8651E-6	3.8651E-6	3.8651E-6
30	3.2945E-6	3.2945E-6	3.2945E-6	3.2945E-6	3.2945E-6	3.2945E-6
40	2.9400E-6	2.9400E-6	2.9400E-6	2.9400E-6	2.9400E-6	2.9400E-6
50	2.6909E-6	2.6909E-6	2.6909E-6	2.6909E-6	2.6909E-6	2.6909E-6

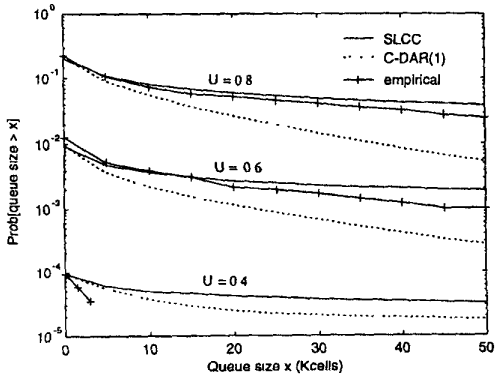

Fig. 6. Queue occupancies for the empirical, SLCC, and C-DAR(1) inputs

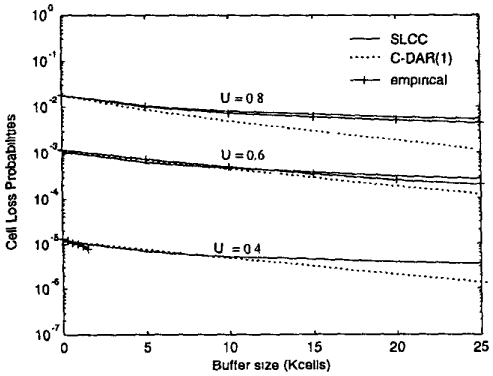

Fig. 7. Cell loss probabilities for the empirical, SLCC, and C-DAR(1) inputs

TABLE V

CELL LOSS PROBABILITIES FOR SUPERPOSED SOURCES (5, 10) AT U = 0.8 (JPEG-CODED *Star Wars*)

Queue Size (cells)	CLPs for 5 superposed sources			CLPs for 10 superposed sources		
	Real	SLCC	C-DAR(1)	Real	SLCC	C-DAR(1)
200	2.7478E-3	3.4878E-3	3.4878E-3	2.6600E-3	3.1957E-3	3.1957E-3
400	7.6870E-4	8.3803E-4	8.3803E-4	5.8069E-4	6.1515E-4	6.1503E-4
600	5.2454E-4	5.2767E-4	5.2767E-4	6.4482E-5	7.1141E-5	7.1087E-5
800	4.1048E-4	5.1766E-4	5.1766E-4	2.1726E-5	3.0801E-5	3.0704E-5
1000	3.7405E-4	5.0800E-4	5.0800E-4	1.6281E-5	2.0480E-5	2.0347E-5
2000	2.9570E-4	4.6720E-4	4.6427E-4	1.3314E-5	1.9038E-5	1.8820E-5
4000	2.1745E-4	4.0787E-4	3.9467E-4	1.0561E-5	1.6780E-5	1.6413E-5
6000	1.6288E-4	3.6560E-4	3.4150E-4	0	1.5128E-5	1.4460E-5
8000	1.1068E-4	3.3398E-4	2.9924E-4	0	1.3870E-5	1.2825E-5
10000	9.4143E-5	3.0948E-4	2.6461E-4	0	1.2882E-5	1.1439E-5
20000	7.8848E-5	2.3939E-4	1.5486E-4	0	1.0006E-5	6.8986E-6
40000	5.6234E-5	1.8287E-4	6.4527E-5	0	7.6595E-6	3.0420E-6
60000	0	1.5589E-4	3.0964E-5	0	6.5347E-6	1.5313E-6
80000	0	1.3912E-4	1.6159E-5	0	5.8343E-6	8.3345E-7
100000	0	1.2734E-4	8.9330E-6	0	5.3416E-6	4.7892E-7

model [15] (a SRD video traffic model) is just a kind of SL process with only exponential tail in the SLCC.

We devised a queueing analysis algorithm named the ***quantization reduction method*** for the SL/D/1/K queueing system. The application to video traffic showed that the quantization reduction method provides efficient and accurate approximation and the upper and lower bounds of the approximation as well. Especially in the SL process input, the algorithm does not suffer from the computational load because in the SL process the dimension of the one-step transition matrix does not depend on the state size of the input process.

Simulation results showed that the SLCC with the proposed parameter matching algorithm consistently provides accurate prediction of the actual queueing performance. In contrast, the C-DAR(1) model, while showing acceptable prediction under most conditions, underestimates the queue occupancy at large queue sizes under a heavy traffic load. The hyperbolic tail at large lags (LRD) strongly affects the probability in large queue sizes, but only slightly in small buffer sizes. This is why we can find many seemingly contradictory arguments on the importance in the literature.

In this paper, we did not give a clear expression for dividing the LRD-dominant region and the SRD-dominant region. It should be noted that the region under which a SRD model works successfully depends on the type of video traffic, especially the video coding algorithm. We will consider this in our future work, where real-time parameter estimation of the SL process and on-line admission control based on the SL process will be studied.

ACKNOWLEDGMENT

We thank Dr. M.W. Garrett, Dr. Bo Ryu, and Dr. O. Rose for making the traces available and Dr. M. R. Frater for his comments on the motivation of this work. Also, H. Ahn would like to thank Ms. J. Scherer for her invaluable discussion on the manuscript.

APPENDIX A: PROOF OF EQUATION (3)

We give a simple and useful derivation of equation (3) different from that in [12], [22]. Mandelbrot [22] gave an expression for the ACF for the discretely distributed duration of T_i. First, we obtain the autocovariance of the stationary process $X(t)$, $Cov(X(\tau), X(\tau+t)) = Cov(X(0), X(t))$ as follows.

$$\begin{aligned} Cov(X(0),X(t)) &= E[(X(0)-\mu_X)(X(t)-\mu_X)] \\ &= E[(X(0)-\mu_X)^2 1_{\{T_1>t\}}] \\ &\quad + E[(X(0)-\mu_X)(X(t)-\mu_X)1_{\{T_1\le t\}}] \\ &= \sigma_X^2 Pr[T_1 > t] \\ &= \sigma_X^2 \frac{1}{\mu_T}\int_t^\infty (1-F_T(y))\,dy. \end{aligned}$$

Then, the relationship between $\rho(t)$ and $F_T(t)$ in the SL process is obtained by

$$\rho(t) = \frac{1}{\mu_T}\int_t^\infty (1-F_T(y))\,dy.$$

APPENDIX B: THE DETAILED FORMULA FOR QUEUEING ANALYSIS

We give detailed formulas for the transition matrices of the queueing system. First, noting that during $[t_n, t_{n+1})$,

input arrives at uniform rate of i cells per frame, the elements of each transition matrix is obtained as follows, respectively, we can obtain the following transition matrices.

$$p^{a}_{(i,l),(j,k)} = \begin{cases} 0, & \text{for } i \geq C, l > k, \\ f_S(j)(F_T\left(\frac{(k-l+\frac{1}{2})h}{(i-C)}\right) - F_T\left(\left(\frac{(k-l-\frac{1}{2})h}{(i-C)}\right)^+\right)), & \\ & \text{for } i \geq C, l \leq k, \\ f_S(j)(F_T\left(\frac{(l-k+\frac{1}{2})h}{(C-i)}\right) - F_T\left(\left(\frac{(l-k-\frac{1}{2})h}{(C-i)}\right)^+\right)), & \\ & \text{for } i > C, l \geq k, \\ 0, & \text{for } i < C, l > k. \end{cases}$$

$$p^{u}_{(i,l),(j,k)} = \begin{cases} 0, & \text{for } i \geq C, l \geq k, \\ f_S(j)(F_T\left(\frac{(k-l)h}{i-C}\right) - F_T\left(\left(\frac{(k-l-1)h}{i-C}\right)^+\right)), & \\ & \text{for } i \geq C, l < k, \\ f_S(j)(F_T\left(\frac{(l-k+1)h}{C-i}\right) - F_T\left(\left(\frac{(l-k)h}{C-i}\right)^+\right)), & \\ & \text{for } i < C, l \geq k \\ 0, & \text{for } i < C, l < k. \end{cases}$$

$$p^{l}_{(i,l),(j,k)} = \begin{cases} 0, & \text{for } i \geq C, l > k, \\ f_S(j)(F_T\left(\frac{(k-l+1)h}{i-C}\right) - F_T\left(\left(\frac{(k-l)h}{i-C}\right)^+\right)), & \\ & \text{for } i \geq C, l \leq k, \\ f_S(j)(F_T\left(\frac{(l-k)h}{C-i}\right) - F_T\left(\left(\frac{(l-k-1)h}{C-i}\right)^+\right)), & \\ & \text{for } i < C, l > k, \\ 0, & \text{for } i < C, l \leq k. \end{cases}$$

REFERENCES

[1] H. Ahn, A. Baiocchi, and J.-K. Kim, "On the time scales in video traffic characterization for queueing behavior," ***Computer Communications,*** vol. 22, pp. 1382-1391, Sep. 1999.

[2] H. Ahn,"The effects of multiple time-scale burstiness and long-range dependence in VBR video traffic on traffic control in multimedia networks," Ph. D. dissertation, Dept. Electrical Engineering, KAIST (Korea Advanced Institute of Science and Technology), Taejon, Korea, Feb., 2000.

[3] A. Baiocchi, N. B. Melazzi, M. Listani, A. Roveri, and R. Winkler, "Loss performance analysis of an ATM multiplexor loaded with high-speed on-off sources," ***IEEE J. Select. Areas in Commun.***, vol 9, no. 5. pp. 388-394, Apr. 1991.

[4] M. S. Bazaraa, H. D. Sherali, and C.M. Shetty, Nonlinear Programming: Theory and Algorithms, Second Edition, John Wiley, New York, 1993.

[5] J. Beran, R. Sherman, M. S. Taqqu, and W. Willinger, "Long-range dependence in variable bit rate video traffic," ***IEEE Trans. Commun.,*** vol. 43. no.2/3/4 pp. 1566-1579, 1995.

[6] A. Elwalid, D. Heyman, T. V. Lakshman, D. Mitra, and A. Wiess, "Fundamental bounds and approximations for ATM multiplexor with applications to video teleconferencing," ***IEEE J. Select. Areas Commun.***, vol. 13, no. 6, pp. 1004-1016, Aug. 1995.

[7] D. Eun, H. Ahn, B. H. Roh, and J.-K. Kim "Effects of long-range dependence of VBR video traffic on queueing performances," ***in Proc. GLOBECOM'97,*** Phoenix, USA, Nov. 1997, pp. 1440-1444.

[8] A. Erramilli, R. Singh, and P. Pruthi, "An approximation of deterministic chaotic maps to model packet traffic," ***Queueing Systems***, vol. 20, pp. 172-206, 1995.

[9] A. Erramilli, O. Narayan, and W. Willinger, "Experimental Queueing Analysis with Long-Range Dependent Packet Traffic," ***IEEE/ACM Trans. Networking,*** vol. 4, no. 2, pp. 209-223 Apr. 1996.

[10] M. R. Frater and J. F. Anold, "A new statistical model for traffic generated by VBR coders for television on the broadband ISDN," ***IEEE Trans. Circuits Syst. Video Technol.***, vol. 4, no. 6, pp. 521-526 Dec. 1994.

[11] M. W. Garrett and W. Willinger, "Analysis, modeling and generation of self-similar VBR video traffic," ***in Proc. ACM SIGCOM'94,*** London, England, Aug. 1994, pp. 269-280.

[12] M. Grasse, M. R. Frater, and J. F. Arnold, "Origins of long-range dependence in variable bit rate video traffic," ***in Proc. ITC-15,*** Washington DC, USA, 23- 27, June, 1997, pp. 1379-1388.

[13] B. Hajek and L. He, "On variations of queue responses for inputs with identical means and autocorrelation functions," ***in Proc. CISS'96,*** Princeton University, Princeton, NJ, Mar. 1996, pp. 1195-1201.

[14] B. Hajek and L. He, "On variations of queue response for inputs with identical means and autocorrelation functions," ***IEEE/ACM Trans. Networking,*** vol. 6, no. 5, pp. 588-598, Oct. 1998.

[15] D. P. Heyman and A. Tabatabai, and T. V Lakshman, "Statistical analysis and simulation study of video teleconferencing traffic in ATM networks," ***IEEE Trans. Circuits Syst. Video Technol.***, vol. 2, no. 1, pp. 49-59 Mar. 1992.

[16] D. P. Heyman and T. V. Lakshman, "What are the implications of long-range dependence for VBR video traffic engineering?," ***IEEE/ACM Trans. Networking,*** vol. 4, no. 3, pp. 301-317 June 1996.

[17] C. Huang, M. Devetsikiotis, I. Lambadaris, and A. R. Kaye, "Modeling and simulation of self-similar variable-bit-rate compressed video: A unified approach," ***in Proc. ACM SIGCOM'95,*** Cambridge, MA, 1995, pp. 114-125.

[18] P. R. Jelenković, A. A. Lazar, and N. Semret, "The effect of multiple time scales and subexponentiality in MPEG video streams on the queueing behavior," ***IEEE J. Select. Areas Commun.***, vol. 15, no. 6, pp. 1052-1071 Aug. 1997.

[19] S.Q.Li, "A new performance measurement for voice transmission in bursty and packet switching," ***IEEE Trans. on Commun.***, vol. 35, no. 10, pp. 1083-1094 Oct. 1987.

[20] S.Q.Li and C. L. Hwang, "Queue response to input correlation functions: Continuous spectral analysis," ***IEEE/ACM Trans. Networking,*** vol. 1, no. 6, pp. 678-692, Dec. 1993.

[21] D. M. Lucantoni, M. F. Neuts, and A. R. Reibman, "Methods for performance evaluation of VBR video traffic models," ***IEEE/ACM Trans. Networking,*** vol. 2, no. 2, pp. 176-180 Apr. 1994.

[22] B. Mandelbrot, "Some noise with 1/f spectrum: a bridge between direct current and white noise," ***IEEE Trans. Information Theory,*** vol. 13, no. 2, pp. 289-298 Apr. 1967.

[23] M. F. Neuts, ***Matrix Geometric solutions in Stochastic Models***, Baltimore, MD: Johns Hopkins University Press, 1981.

[24] I. Norros, "On the use of fractional Brownian motion in the theory of connectionless networks," ***IEEE J. on Select. Areas in Commun.***, vol. 13, no. 6, pp. 953 -962 Aug. 1995.

[25] J. W. Roberts, Ugo Mocci, and Jorma Virtamo Ed., ***Broadband network teletraffic: Final Report of Action COST 242***, Springer, 1996.

[26] O. Rose. "Statistical properties of MPEG video traffic and their impact on traffic modeling in ATM systems," University of Wuerzburg. Institute of Computer Science Research Report Series. Report No. 101. Feb. 1995. ftp address and directory of the used video trace: ftp-info3.informatik.uni-wuerzburg.de/pub/MPEG/

[27] S. M. Ross, ***Stochastic Process***, Reading, 2nd Ed., John Wiley & Sons, 1996. Springer, 1996.

[28] B. Ryu, "Modeling and simulation of broadband satellite networks-Part 2: traffic modeling," ***IEEE Communications Magazine***, pp. 48-56, July 1999.

[29] S. Xu, Z. Huang, and Y. Yao, "A theoretic analysis model for VBR video traffic in ATM networks," ***in Proc. ICC'97,*** Montreal, Canada, May, 1997, pp. 844-848.